Chapter 5

Frequency Response Based Identification Approach

5.1 Introduction: *Transition from the TDR-Based Approach*

This chapter presents the subscriber line identification approach utilizing the frequency response of the local loop. The new procedure is the result of an adaptation of the original time-domain procedure (Chapter 3) to using frequency-domain data and to incorporating the MODE-type algorithm (Chapter 4). Prior to discussing the details of the frequency domain approach, the pros and cons of the TDR and frequency response based procedures are considered.

From Chapter 2, TDR response simulation employs a 2^{15}-point IFFT to combat time-domain aliasing. Even with the utilization of an efficient radix-2 FFT algorithm, the repeated execution of the IFFT for such a large number of data points decimates the speed of the overall time-domain algorithm. Moreover, the incorporation of the MODE-type algorithm — which operates in the frequency-domain — significantly increases the needed number of FFT executions, thereby resulting in an even slower identification procedure. In addition to the increased computational speed, the aliasing effect - which cannot be completely eliminated due to the wideband nature of the transmission line - eventually obscures the reflection data when the reflection node is far away from the measurement node. With frequency-domain data, the need for FFT/IFFT operations and control of aliasing in the simulation are both eliminated. On the other hand, processing frequency-domain data conceals information that is readily observable in the time-domain (*i.e.*, reflections that are well separated). Finally, another consideration independent of the procedure is the accuracy of the actual measurements in a particular domain. Overall, considering how much we can gain, approaching the loop identification in the frequency-domain is quite appealing.

The most important fundamental concept that is mutual in both approaches is the general MODE assumption that the data is a sum of systematically related signals. The TDR response is the sum of

the reflections returning from loop nodes. This idea can be extended to the data in the frequency-domain, as the loop frequency response is the sum of the frequency responses that are responsible for each TDR reflection. Taking another step in association with the MODE-type algorithm, the TDR frequency response measurement can be decomposed into the reflection frequency responses — each responsible for characterizing a TDR reflection (Section 5.2).

The iterative modeling employed in the TDR-based procedure is again used in the frequency response based procedure. Each cycle involves the detection of the loop node and extracting the loop parameters from the detected node. However, the concept that significantly differs from its predecessor is the order in which nodes are processed (Section 5.3).

The MODE-type algorithm essentially replaces the previous WCSSE criterion based reflection detection process. The subsequent node location estimation (length estimation) is tightly related to the estimated reflections or MODE-type estimates. As a result, the node location is much more accurately estimated than the previous WCSSE-based method. To assist the MODE-type estimation process, information theory based criteria [29] for estimation of the number of dominant reflections is also incorporated in the node location estimation process. (Section 5.4) The node parameters are again determined from consideration of all possible candidates. The new decision criterion is the sum of squared error (SSE) over all of the sample frequency points (Section 5.4). The length refinement of each candidate model is accomplished by the minimization of the candidate's SSE with respect to its known length segments (Section 5.6)..

5.2 Decomposition of TP Loop Frequency Response

Recall that the TDR response is defined by the convolution of its input signal and the system impulse response of the subscriber loop, or equivalently expressed as (2-11) in the frequency domain. Furthermore, (2-18) defines the TDR response $y_{TDR}(t)$ as a linear combination of individual reflections $y_n(t)$. Equation (2-18) transformed to transformed to the frequency domain yields

$$Y_{TDR}(f) = \sum_{i=0}^{\infty} Y_{ri}(f) \tag{5-1}$$

where $Y_n(f)$ is the Fourier spectrum of the i-th reflection. Since each individual path on the loop system block diagram defines an individual reflection, the relationship between the input signal and each individual reflection can too be viewed as a system (or subsystem to $H(f)$) and expressed as

$$Y_{ri}(f) = X_{TDR}(f)H_i(f) \tag{5-2}$$

where $H_i(f)$ is the frequency response from the input to the i-th reflection in the system. The system is defined by cascading all of the blocks in the reflection path. Substituting (2-11) and (5-2) into (5-1) yields

$$X_{TDR}(f)H(f) = \sum_{i=0}^{\infty} X_{TDR}(f)H_i(f) \tag{5-3}$$

Dividing both sides of (5-3) by $X_{TDR}(f)$ yields

$$H(f) = \sum_{i=0}^{\infty} H_i(f) \tag{5-4}$$

For example, consider the single segment example (Figure 2-11) in Section 2.6.1. Its TDR response and first four reflections are shown in Figures 2-13 and 2-14, respectively. The corresponding frequency response and first four reflection frequency responses are shown in Figure 5-1. The reflection frequency responses are defined based on (2-19) and (2-20) as

$$H_0(f) = A(f) = \frac{Z_0(f)}{Z_0(f) + Z_g}, \tag{5-5}$$

$$H_1(f) = A(f)\Gamma_{11}(f)\Gamma_{11}(f)e^{-2l_1\gamma_1(f)}, \tag{5-6}$$

$$H_2(f) = A(f)\Gamma_{11}(f)\Gamma_{11}^2(f)e^{-2l_1\gamma_1(f)}, \tag{5-7}$$

and

$$H_3(f) = A(f)\Gamma_{11}(f)\Gamma_{11}^3(f)e^{-2l_1\gamma_1(f)}. \tag{5-8}$$

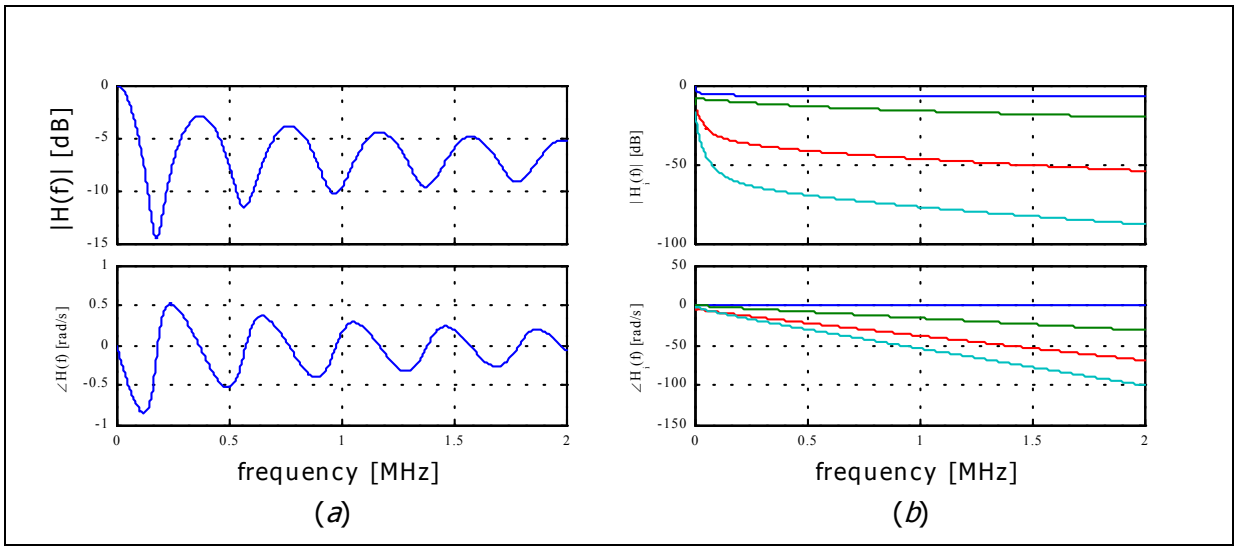

Figure 5-1: Frequency response decomposition (a) and its first three reflection frequency responses (b).

Equation (5-4) and Figure 5-1 together resemble the MODE-type assumption (4-67) with

$$H(f) \equiv \sum_i \alpha_i \rho_i^f \tag{5-9}$$

at high frequencies (> ~1 MHz). This observation is further supported by the analysis performed in Section 4.5 with respect to the individual TP parameters. This implies that the MODE-type algorithm can be applied directly to $H(f)$ by setting $s(t)$ equal to the unit impulse. The MODE-type algorithm's ability to separate reflections and to detect their TOAs will allow us to estimate the corresponding lengths of transmission line segments.

5.3 Frequency Domain Iterative Loop Structure Modeling

The frequency response based algorithm receives as its input sample frequencies and the LUI frequency-response values at those frequency points and returns a loop model that best explains the measurements. The selection of sample frequency points is one of the critical settings for this algorithm. The frequency points must be equally spaced for the MODE-type algorithm. Currently, the frequency range over 1 MHz to 2 MHz, as employed with the MODE-type algorithm in Section 4.7, with 101 equally spaced samples is chosen ($\Delta f = 10$ kHz).

The general iteration procedure is similar to the previous time-domain procedure in Chapter 3. The model is initialized with a measurement node, and each iteration reveals a new node followed by

infinitely long TP segments, if any new segments are created. The first task in each cycle is to separate the reflection frequency responses, followed by estimating the node location and its parameters. If the new node is placed on an infinitely long segment, the segment is replaced with a finite segment. The procedure terminates when no infinitely long TP segment exists in the loop model.

5.3.1 Reflection Processing Order

The most important procedural change, in going from time domain to frequency domain processing, is the order in which the reflections are processed. The frequency domain procedure processes the reflection frequency responses in the order of reflection strength while its time-domain predecessor processed in the order of reflection appearance. Resolving the reflections in the order of appearance is not the most suitable approach in the frequency-domain since all of the reflections interfere with each other over the entire frequency band and the notion of time is completely obscured. On the other hand, processing reflections in order of strength allows the identification process to incorporate the loop node that contributes the most to the overall frequency response.

There is one drawback with the order-by-strength approach. Order-by-appearance guaranteed that all of the reflections of the intermediate partial model are complete. That is, all of the discontinuities (*i.e.* loop nodes) in the reflections' paths exist in the model. Conversely, the order-by-strength approach cannot guarantee such a condition. This could cause a potential mishap that a reflection, of which path is not yet completely defined on a partial model, to be associated with an incorrect loop node.

To demonstrate this issue, consider the TP loop in Figure 5-2a; the first two reflections are illustrated on the reflection diagram. If Segment 2 is sufficiently short[2], the first reflection (dashed) is much weaker than the second reflection (solid). Consequently, the frequency domain approach will find Node 2 before Node 1 and thus constructs the network model in Figure 5-2b in the first reconstruction cycle. The estimated length of the modeled Segment 1 is roughly the sum of the lengths of the actual Segments 1 and 2. The difference between the two loops and reflection diagram pairs immediately tells us that a reflection from Node 2 would not be the same as a reflection from Modeled Node 1. As the reflection diagram indicates, the reflection path for Node 2 contains a pair of transmissions over the discontinuity of Node 1 and propagates through two different types of cables, while the reflection path for Modeled Node 2 only consists of a single propagation medium and no

[2] In general, ~600 m. is the threshold for the condition for data sampled over the 1 MHz to 2 MHz region. The threshold is highly frequency dependent.

discontinuity. The magnitude responses that are responsible for the two reflections are shown in Figure 5-2c where the difference is clearly illustrated.

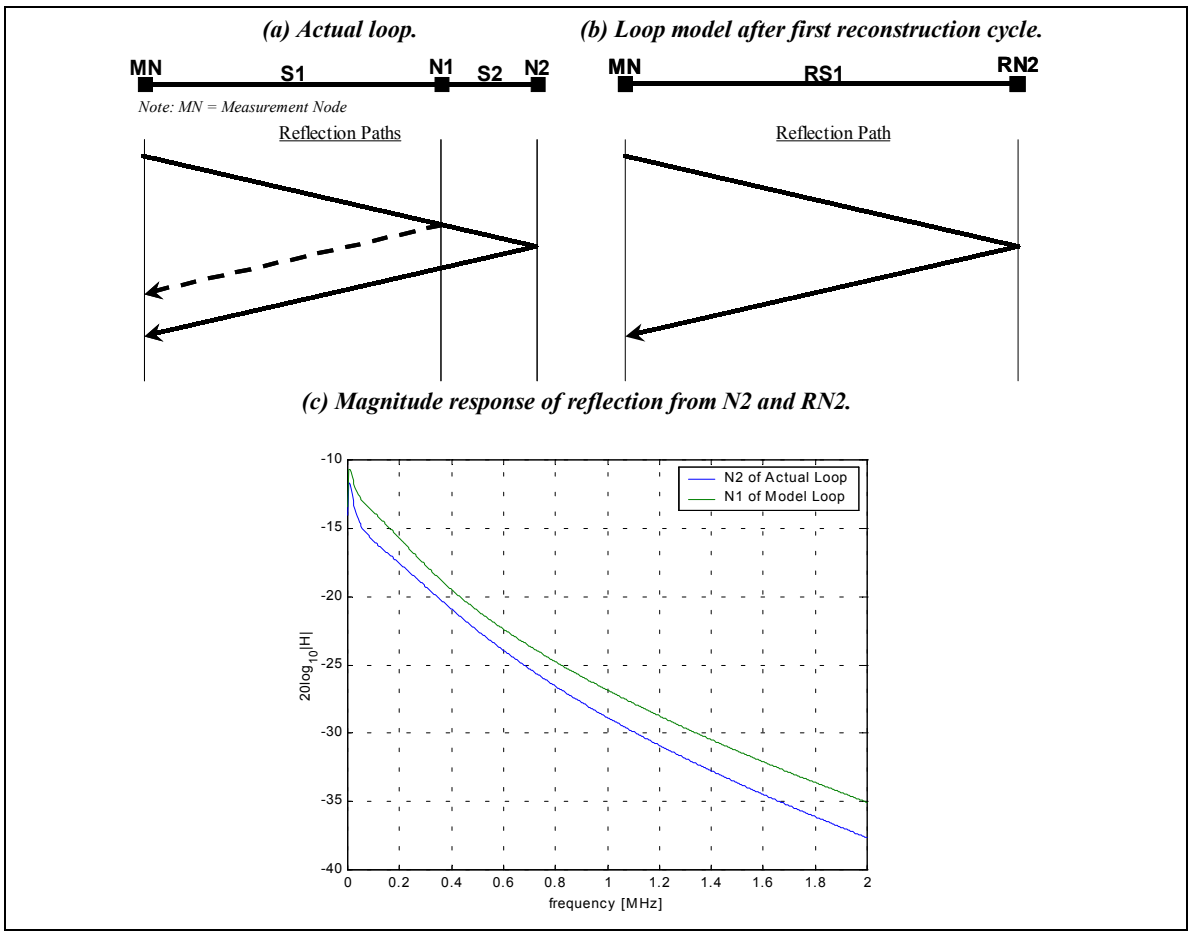

Figure 5-2: An illustration of mismatch between actual and model reflections based the strongest-reflection first approach (by skipping over a GC node).

The latter phenomenon forces an increase in the number of candidate models for each process cycle. In addition to the existing nine standard candidates for an infinitely long segment, an additional set of candidate models must be considered on the finite segment(s) to ensure that there is no missing weaker node.

5.4 Node Location Estimation (Length Estimation)

The previously separate reflection (node) detection procedures and segment length estimation procedures are unified in the frequency domain identification approach. The MODE-type algorithm is employed to separate the reflection frequency responses or equivalently to detect potential loop

node locations. The length estimation is obtained from the MODE-type estimates of the phase angles — m_β in (4-64) — of the reflection frequency responses. While there is theoretically an infinite number of returning reflections, only a few reflections — the dominant ones — are actually detected by the algorithm. Mathematically the MODE-type estimates

$$\widetilde{H}(f) \approx \sum_{l=1}^{L} \hat{\alpha}_l \hat{\rho}_l^{\,f} \tag{5-10}$$

where $\widetilde{H}(f)$ defines the LUI frequency response after removal of known information, L is the estimated number of unknown dominant reflections, and $\hat{\alpha}_l$ and $\hat{\rho}_l$ — both complex quantities — are the scaling and damping factor estimates, respectively, for the l-th mode. Out of the L relevant MODE estimates, we are interested in an estimate that corresponds to the unresolved reflection with the strongest energy level. Subsequently, the MODE-type estimates are converted into a length estimate for the segment(s) leading to the possible new node. To summarize, there are four steps involved in the length estimation process:

1. Data pre-processing — removal of known information,
2. Estimation of the number of dominant reflections in the residual data,
3. Conversion of the MODE-type algorithm estimates to segment lengths, and
4. Selection of the probable length estimate corresponding to the next strongest reflection.

The following subsections discuss each aspect of the procedure.

5.4.1 Data Pre-Processing

The reflections, in general, weaken exponentially with respect to their path distances. The reflections from far-out nodes can be so insignificant relative to the much stronger reflections from near nodes that the MODE algorithm does not detect the far reflections. Therefore, removal, from $H(f)$, of already determined reflections is essential to focus better on the remaining reflections. Moreover, further removal of known information from the remaining frequency response — to isolate its dependence on segment length — results in more accurate length estimation.

The length estimation procedure receives three pieces of information: the LUI frequency response $H(f)$, a partially reconstructed model, and a processing node at which the next segment's relative length is found. The processing node is defined as a node that spawns an infinitely long segment. The

first step is the simulation of the partial model's frequency response $\hat{H}(f)$. Assuming the partial network model is correct thus far, the model error

$$H_e(f) = H(f) - \hat{H}(f) \tag{5-11}$$

contains all of the unidentified reflection frequency responses.

While employing the MODE-type algorithm to $H_e(f)$ is a valid operation, more accurate length estimations can be obtained by further data pre-processing. All known information for the reflection path (*i.e.* the transmission and reflection coefficients of known discontinuities and signal propagation functions over the already determined segments) can be removed from $H_e(f)$.

Consider the simple case of estimating the length of a single segment of which the first four reflections are analytically defined in (5-5) – (5-8). The LUI frequency response decomposition is

$$H(f) = A(f) + A(f)\mathrm{T}_{11}(f)e^{-2l_1\gamma_1(f)} + A(f)\mathrm{T}_{11}(f)\Gamma_{11}(f)e^{-4l_1\gamma_1(f)}\cdots \tag{5-12}$$

After the first iteration and just prior to length estimation, the partial model consists of an infinitely long TP segment (note that $Z_0(f)$ and $\gamma(f)$ are already known); and the model frequency response is

$$\hat{H}(f) = A(f) \tag{5-13}$$

or the first term of the LUI response. Consequently,

$$H_e(f) = A(f)\mathrm{T}_{11}(f)e^{-2\gamma_1(f)l_1} + A(f)\mathrm{T}_{11}(f)\Gamma_{11}(f)e^{-4\gamma_1(f)l_1} + \cdots. \tag{5-14}$$

In other words, $H_e(f)$ is responsible for the sum of all of the reflections excluding the first reflection $H_0(f)$. Both $A(f)$ and $\mathrm{T}_{11}(f)$ can be derived from the current model and consequently can be removed since they are not functions of segment length. Removal of these terms yields

$$\tilde{H}(f) = \frac{H_e(f)}{A(f)\mathrm{T}_{11}(f)} = e^{-2l_1\gamma_1(f)} + \Gamma_{11}(f)e^{-4l_1\gamma_1(f)} + \cdots \tag{5-15}$$

Note that the first term of $\widetilde{H}(f)$ is $e^{-2\gamma(f)l}$ which only consists of the length and propagation function of the segment. This first term corresponds to the next strongest reflection in this particular example. With the MODE-type algorithm, an estimate for $e^{-2/_1\gamma_1(f)}$ can be obtained, and subsequently the length can be determined in least-squares fashion.

In general, the known information to remove (*i.e.*, $A(f)\mathrm{T}_{11}(f)$ in the above example) can be obtained by cascading all of the known components in the reflection. In the example, most of the components of $H_1(f)$ — the first reflection from Node 2 — are already known, except for the propagation term, after the identification of Node 1.

5.4.2 Determination of the Number of Dominant Reflections

Although the number of signals that are overlapping is a required input to the MODE-type algorithm, the subscriber loop responses theoretically produce an infinite number of reflections. The reflection strength weakens exponentially as its path distance increases. Therefore, the MODE algorithm can only detect a dominant subset of all reflections.

Thus, the estimated number of dominant reflections (ENDR) $\hat{L}_0$ needs to be determined prior to using the MODE algorithm. The information theoretic criterion technique [29] is employed for this estimation task. Similar to the MODE-type algorithm, this procedure is also based on eigenanalysis and was originally developed for sensor array processing. Two criteria are used with our routine: the Akaike information criterion (AIC) and the minimum description length criterion (MDL).

The algorithm is based on the correlation matrix $\hat{\mathbf{R}}_d^{(m)}$ in (4-75) for varying snapshot size *m*. For $m \in \{3,\ 4,\ \ldots,\ \lfloor N/3 \rfloor\}$ where *N* is the length of the observed data record, compute $\hat{L}_0^{(m)}$ from the AIC and MDL criteria as follows:

1. Compute the eigenvalues $\lambda_1 > \lambda_2 > \cdots > \lambda_m$ of $\hat{\mathbf{R}}_d^{(m)}$.
2. For all possible numbers of reflections $k \in \{0,\ 1,\ \ldots,\ m-1\}$, compute the criteria:

$$AIC_k^{(m)} = -2\ln\left(\frac{\prod_{i=k+1}^{m}\lambda_i^{1/(m-k)}}{\frac{1}{m-k}\sum_{i=k+1}^{m}\lambda_i}\right)^{(m-k)M} + 2k(2m-k)+1 \qquad (5\text{-}16)$$

and

$$MDL_k^{(m)} = -\ln\left(\frac{\prod_{i=k+1}^{m}\lambda_i^{1/(m-k)}}{\frac{1}{m-k}\sum_{i=k+1}^{m}\lambda_i}\right)^{(m-k)M} + \frac{1}{2}k(2m-k)\ln M \qquad (5\text{-}17)$$

where M is the number of snapshots.

3. For snapshot size m, determine $\hat{L}_0^{(m)}$ by selecting the lower of the values of k that minimize AIC and that minimize MDL.

The ENDR $\hat{L}_0$ is the most consistent, or most frequently occurring, estimate for all $\hat{L}_0^{(m)}$ for different m.

To illustrate the process, consider the CSA #1 loop measured from Node 4 with Z_g = 120 Ω. For simplicity, compute the ENDR in the frequency response without the data pre-processing step. The ENDR $\hat{L}_0^{(p)}$ equals 3. This implies that the reflections from Node 4 (0 ft. from Node 4), the tapped node (1,800 ft. from Node 4), and the node at the end of the bridged-tap (2,400 ft. from Node 4) are considered dominant; and all other reflections, including the initial reflection from Node 1 (7,700 ft. from Node 4), are much weaker. Figure 5-3 illustrates some of this selection process. Figure 5-3a is a plot of the MDL for varying k for all m's; most cases minimize at m equal to 3 or 4. Over k = 0:2, both criteria are ∞, indicating insufficient order. Figure 5-3b is the result of all iterations and clearly shows that $\hat{L}_0^{(m)} = 3$ appears most often.

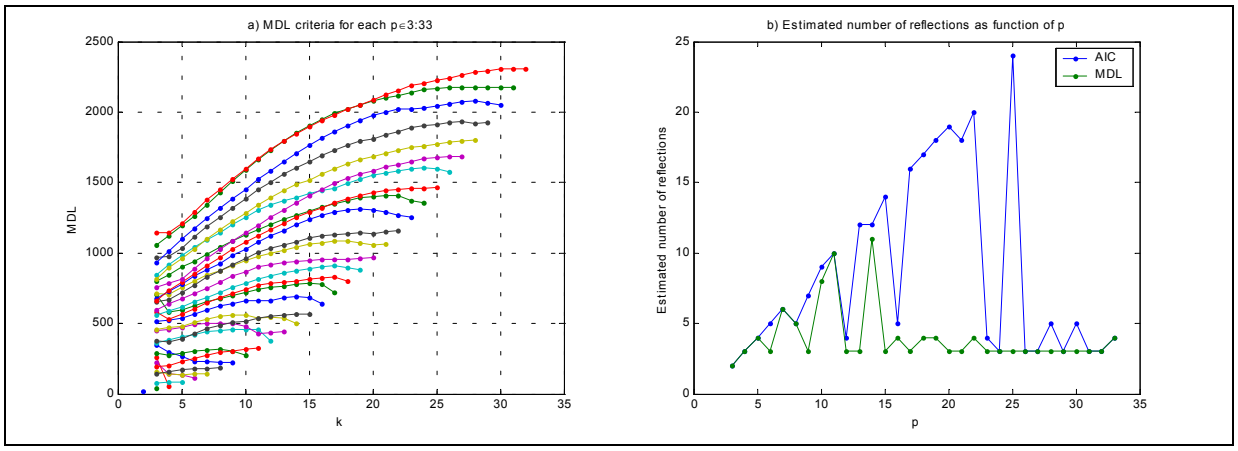

Figure 5-3: MDL Criterion as function of k for all m ∈ 3:33 (a) and estimated number of reflections for all m (b). Note k = 0:2 in (a) are ∞ for most cases.

5.4.3 Conversion of MODE-Type Estimates to Length Estimates

With the information obtained in Section 5.4.1 and 5.4.2 — $\widetilde{H}(f)$ and $\hat{L}_0$ — the MODE-type algorithm has all information necessary for execution. The resulting estimates $\{\hat{\alpha}_l, \hat{\rho}_l\}$ need to be converted to a length estimate $\hat{l}_l$. In previous studies of the MODE-WRELAX and MODE-type algorithms, the phase angles $\angle\hat{\rho}_l$ are first converted to the delays $\hat{\tau}_l$ of the reflections using (4-43). According to the TDR-based approach, $\hat{\tau}_l$ then is converted to $\hat{l}_l$ using the approximated group velocity $\hat{u}_g$ as expressed in (3-8). While this approach would still work under the frequency response approach, it is not the most efficient and accurate way to obtain $\hat{l}_l$. Alternatively, we can look to the TP loop electrical properties instead.

To proceed, first make the following assumption: both the reflection and transmission functions of the TP loop have minimal effects on the reflection phase response $\angle H_i(f)$. This assumption is generally true if the segment length is long, and only high-frequency measurements are considered. With the assumption, $\angle H_i(f)$ is said to be independent of the reflection and transmission coefficients and only dependent on the segment lengths and propagation functions $\gamma(f)$, or simply the exponential terms in the form of $e^{-2l\gamma(f)}$. Equation (5-15) in the above single segment example is the extreme case where the strongest term only contains an exponential term, *i.e.*, one length estimate. In general, the strongest term can have an additional reflection coefficient from the end, if it is not terminated. With this assumption, we can approximate each reflection response as

$$\angle H_i(f) \approx \angle e^{-2\hat{l}_i\gamma(f)} = \angle e^{-2\hat{l}_i[\alpha(f)+j\beta(f)]} = e^{-j2\hat{l}_i\beta(f)} \tag{5-18}$$

The MODE algorithm estimates the left hand side of (5-18) as

$$\angle H_i(f) \approx \angle\tilde{\alpha}\tilde{\rho}^{\frac{f}{\Delta f}} = \angle\hat{\alpha}\hat{\rho}^{f} = e^{j(\hat{\alpha}+\hat{\rho}^{f})} \tag{5-19}$$

where Δf is the frequency sample spacing. Substituting (5-19) into (5-18) yields

$$\angle\alpha_i + f\angle\rho_i = -2\hat{l}_i\beta(f) \tag{5-20}$$

In Section 4.5, $\beta(f)$ is verified to be affine over a limited frequency range. Furthermore, we defined its affine estimate $\hat{\beta}(f) = m_\beta f + c_\beta$ in (4-64). Substituting (4-64) into (5-20) yields

$$\angle\alpha_i + f\angle\rho_i = -2\hat{l}_i(c_\beta - m_\beta f) \tag{5-21}$$

This implies that the length estimate can be obtained from either $\angle\alpha_i$ or $\angle\rho_i$. Since $\beta(f)$ is close to linear ($c_\beta \approx 0$), deriving $\hat{l}_i$ from $\angle\alpha_i$ is not desirable due to division by a small number. Thus, we solve for $\hat{l}_i$ from $\angle\rho_i$:

$$\hat{l}_i = -\frac{\angle\hat{\rho}_i}{2m_\beta} \tag{5-22}$$

A database of m_β, for all possible line types - under consideration in the identification process - and over the LUI data frequency range - must be constructed and be available to the length estimation procedure. It has been determined to be sufficiently accurate to obtain the slope m_β by a simple least-squares fit.

5.4.4 Length Estimate Selection: Based on Estimate Recurrence and Reflection Strength

With $\angle\rho_i$ and using (5-22), a set of lengths estimates $\{\hat{l}_l\}_{l=1}^{\hat{L}}$ can be computed from the MODE-type phase slope estimates. The final objective of the length estimation process is to obtain length estimates that correspond to potential reflections and to eliminate unreliable length estimates. There are two criteria involved in this task:

- Reflection energy estimates, and
- Recurrence of length estimates.

In other words, we would like to select the length estimate that corresponds to the strongest reflection that appears consistently in the MODE estimates with the ENDR $\hat{L} = \{\hat{L}_0 \quad \hat{L}_0 + 1 \quad \cdots \quad \hat{L}_0 + L_{\max}\}$ (currently, $L_{\max} = 3$). The reflection energy over the data frequency range is estimated from the MODE-type magnitude estimates, namely $|\alpha_l|$ and $|\rho_l|$, as follows

$$\hat{E}_l = \sum_{f \in M_f} |\alpha_l|^2 |\rho_l|^{2f} \tag{5-23}$$

The second criterion, the recurrence of the estimate, is determined by successive MODE-type estimations with various ENDRs. A consistently occurring estimate for multiple ENDRs indicates that the estimate does indeed belong. Conversely, an estimate, which appears in less than half of the multiple MODE-type estimation results, is more likely to be a false alarm. This check is especially aimed at reducing the risk of underestimated ENDR. The recurrence check is implemented using the *k*-mean algorithm [30], [31] with a slight modification to cluster the length estimates. The modification involves incorporation of a cluster radius limit and an adaptation mechanism to assign all estimates to a cluster.

Given $\tilde{H}(f)$ and $\hat{L}_0$ from Sections 5.4.1 and 5.4.2, the final steps of length estimation are implemented as follows:

1. For each $\hat{L} = \{\hat{L}_0 \quad \hat{L}_0 + 1 \quad \cdots \quad \hat{L}_0 + L_{\max}\}$, run the MODE-type algorithm and compute $\{\hat{l}_l, \hat{E}_l\}_{l=1}^{\hat{L}}$ from (5-22) and (5-23), resulting in $\hat{L}_0 + L_{\max}(\hat{L}_0 + 1)$ total number of estimate pairs.
2. Remove the length estimates that are out-of-range, *e.g.*, negative length estimates.

3. *Recurrence Check*. Cluster the estimates with respect to length. The cluster diameter is limited to some absolute tolerance (currently set to 100 ft.). Reject clusters that contain fewer than $L_{\max}/2$ estimates. For each remaining cluster, the centroid is taken as the representative estimate to serve as a potential length estimate.
4. *Energy Strength Check*. Select the strongest centroid as the primary reflection candidate, and if there exists another centroid within 20 dB of the primary reflection energy, select it as the secondary reflection candidate. Return the length estimates of these candidates (two estimates are selected to avoid detection of residuals from previously determined segments).

5.5 Node Candidate Generation/Selection

The candidate model selection process (Section 3.4.3) in the TDR-based identification method is — with a few minor changes — maintained in its original form. In the time-domain approach, a pool of candidate models portraying possible configurations for the new node is constructed first, followed by the length refinement on each candidate. The subsequent selection process chooses the best candidate model as the new partial model, i.e. for the next iteration. The best model is the candidate model that minimizes the WSSE criterion (3-13).

The same three-step concept is applied in the frequency-response approach. Instead of over-time-samples, we now use the sum of squared errors over frequency-domain sample points:

$$SSE = \sum_{k \in \text{all sample points}} \left| H_k - \hat{H}_k \right|^2 \tag{5-24}$$

where H_k and $\hat{H}_k$ are the samples of the LUI and model frequency responses, respectively. Note that since $H(f)$ is a complex function, only the magnitude of the error $E_k = H_k - \hat{H}_k$ is taken into consideration.

Candidate models with the new node on an infinitely long segment are still the same nine node configurations as in the time-domain generation process (shown in Figure 3-16). On the other hand, if the new node is on a finite segment, another set of candidates needs to be considered. Two modifications are made:

- The termination node type is not viable when another node follows the new node.

- All nine BT line types need to be considered. One following segment has finite and the other infinite lengths. The two are no longer identical.

These two scenarios are shown in Figure 5-4.

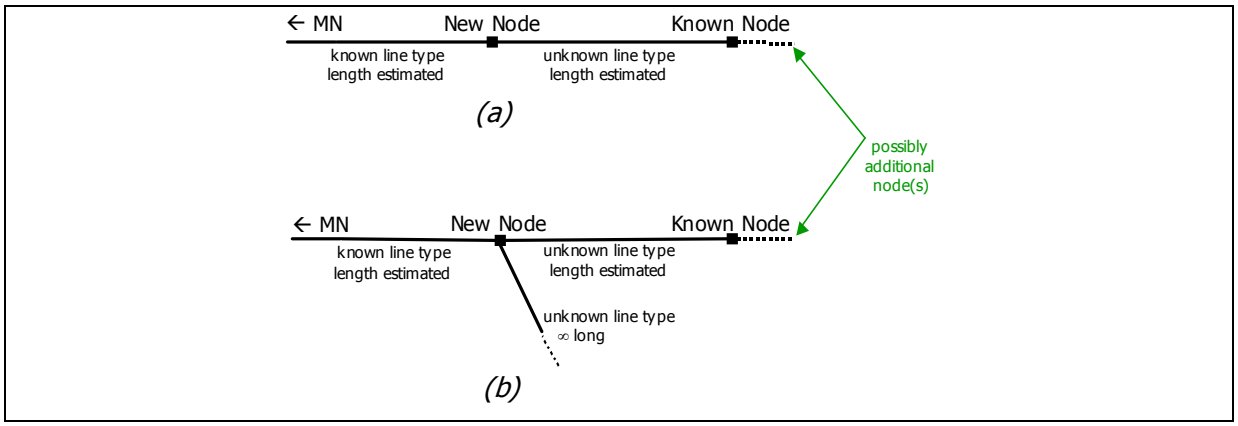

Figure 5-4: Possible node types when new node is inserted in between two existing model nodes. GC (a) and BT(b); Termination is no longer an option.

Let's apply frequency-response based identification to the scenario used in the gauge change example in Section 3.4.2. After the second iteration, the loop model consists of one TP segment with the TP type of Segment 1 and length approximately equal to the sum of two segment lengths (498.08 m) (as shown in Figure 5-5). Despite the fact that the model contains no more infinitely long segments, the identification procedure runs another iteration to check for a possible missing node before terminating its cycle. In the third iteration Node 2 is detected with its length estimate approximately equal to the actual Segment 1 (152.25 m). The newly found node has 11 possible configurations as shown in Figure 3-16.

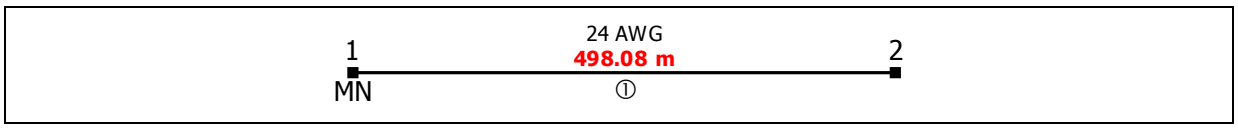

Figure 5-5: Model loop after the second iteration of the GC example in Figure 3-11 with the frequency-response-based approach. The GC node has been neglected.

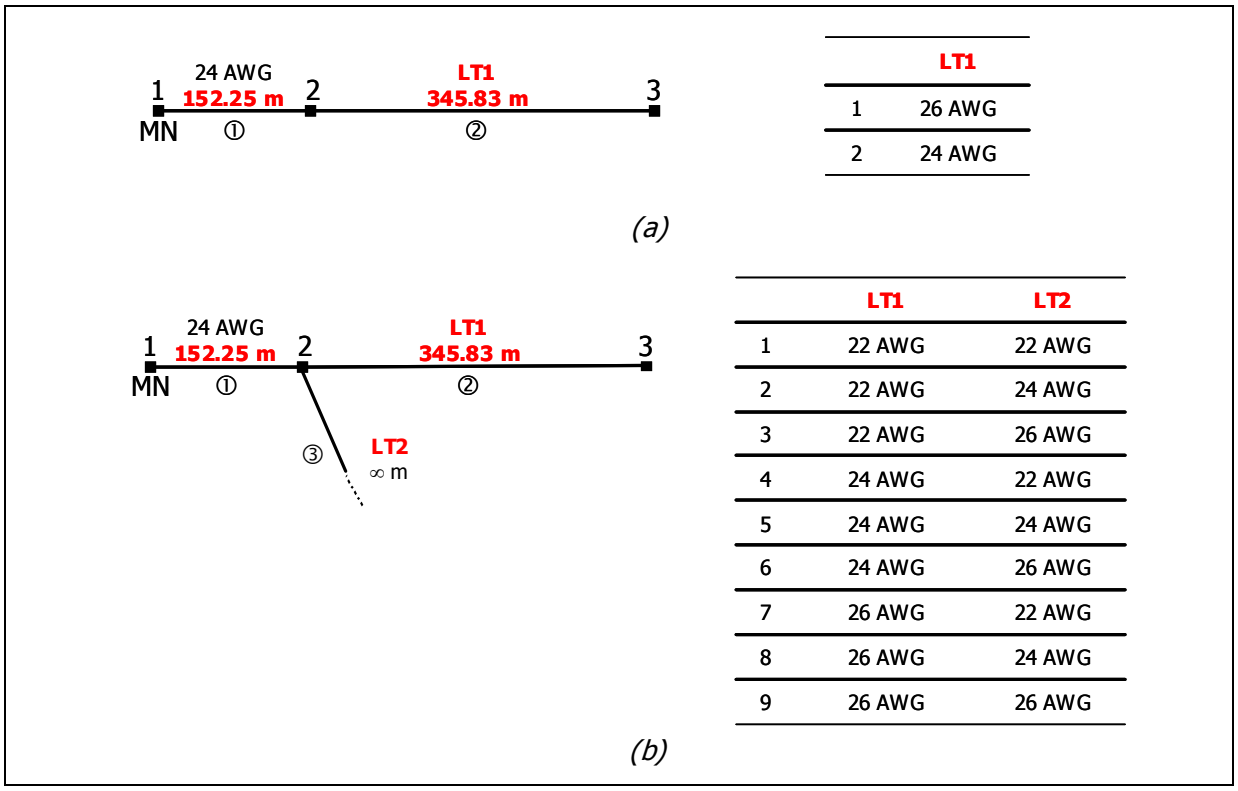

	LT1
1	26 AWG
2	24 AWG

	LT1	LT2
1	22 AWG	22 AWG
2	22 AWG	24 AWG
3	22 AWG	26 AWG
4	24 AWG	22 AWG
5	24 AWG	24 AWG
6	24 AWG	26 AWG
7	26 AWG	22 AWG
8	26 AWG	24 AWG
9	26 AWG	26 AWG

Figure 5-6: All potential node configurations given Figure 5-5 and new length estimate of 152.25 m relative to Node 1. The tables indicate possible line types.

5.6 Length Refinement: Quasi-Newton Optimization

The length refinement method, used to refine the candidate models prior to their selection, also requires a significant modification from its time-domain counterpart. The length refinement procedure is the essential part of the identification that facilitates high-resolution reconstruction, and it is also the most computationally intensive part.

Since the LUI nodes are identified in the order of reflection strength, the optimal segment length (which may not equal the actual length before the entire loop structure has been identified) can be obtained by minimizing the SSE (5-24) of the loop model with respect to the length of the TP segment that leads to the new node. To enhance the result even more, all of the known segment lengths can be adjusted simultaneously by minimizing the SSE in a multi-dimensional minimization process.

The challenge in this approach is that the SSE as a function of model segment length(s) is highly multi-modal in nature, as illustrated in Figure 5-7. However, from good initial lengths (such as the

ones provided by the MODE-type algorithm) together with the correct network model, the closest local minimum to the initial lengths is more likely to be the global minimum.

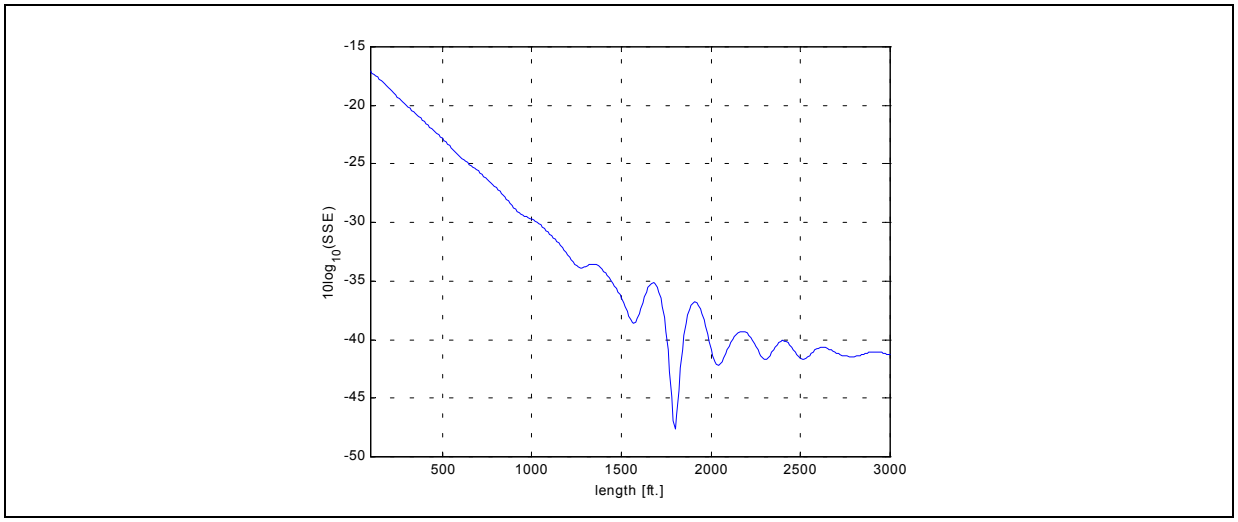

Figure 5-7: Illustration of multimodal nature of SSE.

To implement the minimization process, the quasi-Newton minimization algorithm [32], [33] is employed. Even though this algorithm is usually not suitable for multi-modal minimization problems, the abovementioned reasonable initialization with MODE-type algorithm results enables the quasi-Newton algorithm to be successful. Unlike the correlation-based refinement — which accuracy was limited by the correlation lag index interval — this procedure allows the model to exactly match the LUI in a noiseless environment.

5.7 Summary

This chapter discusses the subscriber line identification approach utilizing the frequency response of the local loop. The motivation behind the change of the measurement data type is to incorporate the MODE-type algorithm, which operates in the frequency-domain, in the identification process in order to detect two closely located loop nodes (in a temporal sense). The loop frequency response can be decomposed into the reflection frequency responses, and each reflection frequency response possesses approximately the characteristics that MODE-type requires for individual superimposed signals.

The proposed frequency-domain procedure is, in most parts, much like its time-domain counterpart, involving first the estimation of the loop node location (segment length) and then

estimating the node parameters through assessing all of its possibilities. The main difference from its predecessor is that the processing order of the nodes is in the order of reflection strength instead of in the order of (temporal) reflection appearance.

The MODE-type algorithm is able to provide two pieces of information from the LUI measurement data: estimated node distances relative to the reference node (5-23) and estimates of the relative reflection strength(5-24). To assist the MODE-type algorithm, two additional techniques are introduced: the information theoretic criterion technique and the *k*-mean based clustering algorithm. AIC and MDL, two information theoretic criteria, are used to obtain the ENDR; which is a necessary piece of data for the MODE-type algorithm. On the other hand, the clustering algorithm is used to post-process the MODE-type estimates to determine the strongest and most consistently recurring estimate.

Additionally, with a change in the working domain, the new decision criterion SSE (5-24) is established for candidate selection as well as for refinement of the model's segment lengths. The length refinement is achieved by utilizing the quasi-Newton minimization algorithm to minimize (5-24) with respect to the model segment lengths.